ACI MATERIALS JOURNAL TECHNICAL PAPER

Title no. 105-M38

Properties of Concrete after High-Temperature Heating and Cooling

by Jaesung Lee, Yunping Xi, and Kaspar Willam

Previous experimental studies on concrete under high temperatures have mainly concentrated on the reduction of stiffness and strength properties. Various experimental parameters have been examined such as maximum temperature, heating rate, types of aggregates used, various binding materials, and loading paths (that is, mechanical loading applied before, during, and after high temperature testing). There exist few data on strength, stiffness, and permeability of concrete considering cooling rate after fire damage, however. Particularly, the increase of permeability severely affects the durability properties of concrete and reduces the remaining service life of the concrete structure. The purpose of this study is to investigate strength, stiffness, and permeability properties of concrete cylinders that are subjected to various heating and cooling scenarios. The thermal diffusivity, weight losses, color changes, and cracks of the specimens are also reported.

Keywords: permeability; stiffness; strength; temperature.

INTRODUCTION

Fire is a great risk to human life, especially in the aftermath of vehicular, earthquake, and other extraneous accidents. When a concrete structure is exposed to fire, the concrete experiences large volume changes resulting from thermal dilatation of aggregate, shrinkage of the cement paste, and spalling due to high thermal stresses combined with internal pore pressure buildup. During a fire, the concrete structure suffers from severe degradation of mechanical and transport properties that may lead to expeditious reduction of the remaining service life. The level of thermal damage depends on the size of the structural member and the spatial and temporal fire conditions such as maximum temperature, heating rate, exposure time, and cooling rate. Therefore, it is very important to study the residual mechanical and transport properties after the concrete was subjected to high temperatures with different heating and cooling rates. A better understanding of these degradation effects will provide essential information to the concrete industry to improve the fire resistance of concrete and to quantify the level of fire damage in the remaining structure.

Extensive experimental studies on various properties of concrete under high temperature have been conducted with an emphasis on the effect of high temperature on the stiffness, strength, and thermal expansion of concrete.[1-21] Very little research has been performed on the reduction of transport properties after concrete is exposed to high temperature, which is very important to the residual durability of concrete. Only recently, Poon et al.[18] conducted an experimental study on the strength and durability of normal- and high-strength concretes. Their study, however, did not consider the effects of heating and cooling rates, which are very important factors on the degradation of concrete due to fire.

From stiffness and strength points of view, not only the heating rate and maximum temperature but also the cooling rate has a strong effect on residual mechanical properties, as well as residual transport properties such as the water permeability. The effect of cooling rate has not been studied systematically in previous studies.

In this paper, some of important mechanical and transport properties of concrete were experimentally studied, including residual stiffness, compressive strength, and water permeability. In addition, thermal diffusivity and weight losses of the concrete specimens were also investigated with different heating and cooling treatments.

RESEARCH SIGNIFICANCE

On the one hand, understanding how damage accumulates and properties vary when the concrete is exposed to high temperature is essential to enhance the fire resistance of reinforced concrete structures (RCS). On the other hand, during a fire, different parts of a concrete structure experience different heating and cooling scenarios. Hence, the material properties of the concrete experiencing different temperature scenarios are significantly different and need to be assessed before a decision is made to repair or rebuild the structure.

SPECIMEN PREPARATION, TESTING METHODS, AND TEST VARIABLES

Mixture design and specimen preparation

In this experimental study, Type I/II portland cement and crushed granite were used to prepare concrete specimens. The bulk specific gravity of the aggregates was 2.69. Concrete admixtures were not used because the focus of this study was to investigate the effect of heating and cooling on concrete made of granite aggregate without considering the effect of admixtures. In the initial mixture design, the water-cement ratio (*w/c*) was 0.50. The mixture was very dry, however, and the *w/c* was adjusted to 0.71 (refer to Table 1). This was due to the fact that the crushed granite sand contains very dry and fine particles. In the project, different *w/c* were examined for workability and 0.71 was the lowest value with which the proper workability with a slump of 1.5 in. (38.10 mm) could be obtained. The moisture content of the aggregates was measured using Test Method B in ASTM D2216. The absorption capacity of aggregates was 0.78%. By subtracting the water absorption capacity of the aggregates from the initial water content, a final *w/c* of 0.67 is obtained. The maximum size of coarse aggregate was 3/4 in. (19.05 mm).

Concrete cylinders with dimensions of 4 x 8 in. (101.6 x 203.2 mm) were prepared for the experimental study. The

ACI Materials Journal, V. 105, No. 4, July-August 2008.
MS No. M-2006-336.R1 received May 2, 2007, and reviewed under Institute publication policies. Copyright © 2008, American Concrete Institute. All rights reserved, including the making of copies unless permission is obtained from the copyright proprietors. Pertinent discussion including authors' closure, if any, will be published in the May-June 2009 *ACI Materials Journal* if the discussion is received by February 1, 2009.

Jaesung Lee *is a Senior Researcher in the Research Department of Building Systems at the Research Institute of Industrial Science & Technology (RIST), South Korea. He received his PhD from the University of Colorado at Boulder, Boulder, CO. His research interests include experimental and theoretical studies of materials and structures subjected to high temperatures, and properties of rubber-modified concrete.*

Yunping Xi *is a Professor in the Department of Civil, Environmental and Architectural Engineering at the University of Colorado at Boulder. He received his PhD from Northwestern University, Evanston, IL. His research interests include experimental and theoretical studies on the durability of construction materials, and conversion of solid waste to construction materials.*

Kaspar Willam *is a Professor in the Department of Civil, Environmental and Architectural Engineering at University of Colorado at Boulder. He received his PhD from the University of California at Berkeley, Berkeley, CA. His research interests include computational mechanics, finite-element analysis of transient and nonlinear problems, and constitutive modeling of nonlinear and inelastic concrete behavior.*

specimens were cured under standard conditions (temperature 73.4 °F [23 °C]; relative humidity [RH] 93%) for 8 weeks in a fog room. For the weight loss and water permeability tests, 4 x 2 in. (101.6 x 50.8 mm) slices were needed. To prepare the permeability specimens, concrete cylinders were cured for 21 days in the fog room and then cut into slices. To make the cuts from 4 x 8 in. (101.6 x 203.2 mm) cylinders, the bottom and top 1.5 in. (38.1 mm) of the specimens were removed. The remaining portion of the cylinders was cut in half and then put into the fog room for another 5 weeks of curing.

Heating and other testing methods

An electrically heated furnace designed for maximum temperature T_{max} = 2912 °F (1600 °C) was used. The interior size of the furnace is 7.8 (width) x 11.4 (depth) x 6.6 in. (height) (198.12 x 289.56 x 167.64 mm). The temperature history inside the furnace was measured and recorded with Type K thermocouples. A data logger was used along with the thermocouples.

To measure temperature distribution in the concrete cylinders, several thermocouples were used. One of the thermocouples measured the ambient temperature between the specimen and the mullite hollow tube (which will be described later in detail), and four Type K thermocouples were installed inside and on the surface of the specimen to measure the temperature distribution inside the concrete cylinder. To fix the position of the thermocouple in the concrete cylinder, the thermocouple wires were shielded by a ceramic thermocouple insulator with two openings. Before placing fresh concrete, the thermocouples were tethered in the cylindrical plastic mold using threads. Figure 1 shows the locations of the thermocouples and the specimen geometry. During the test, the heating rate was 33.8 °F/minute (1 °C/minute), the maximum temperature was 1652 °F (900 °C), the holding time at the maximum temperature was 2 hours, and the default cooling method was natural cooling.

Water permeability, a measurement of the transport property of concrete, provides an excellent indicator for the change of microstructure in concrete under different temperature treatments. The experimental apparatus shown in Fig. 2 was used for measuring water permeability of concrete.[22] The flow of water was measured from the drop of water level in the pipette during the test. The water level was filled to the original level periodically. After the specimen was exposed to a desired temperature scenario, it was placed in an air vacuum for 3 hours to remove air in the specimen, and then it was placed in a water vacuum for 1 hour. The water used for the water vacuum was boiled to make sure it was free of air and then it was cooled to room temperature. The specimens were then immersed for 18 hours in the de-aerated water and finally placed in the water permeability apparatus. The vacuum process follows ASTM C1202.

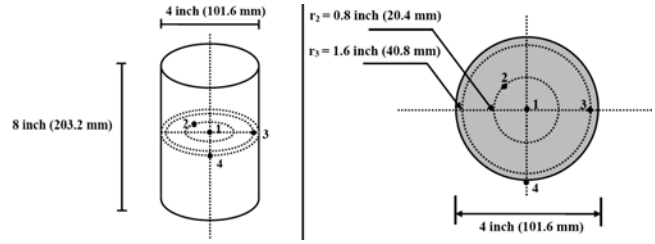

Fig. 1—Locations of thermocouples in a specimen and the specimen geometry.

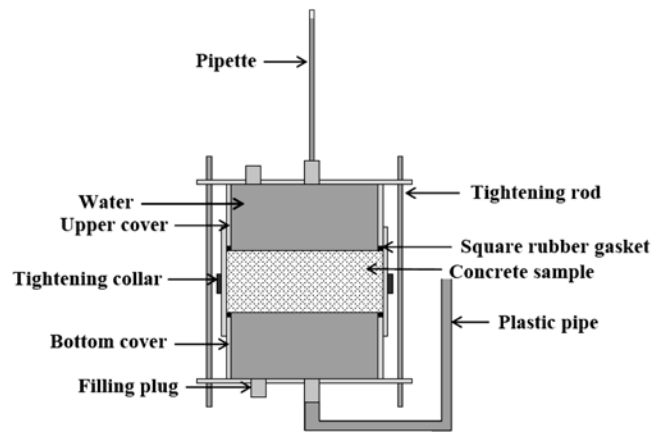

Fig. 2—Experimental setup for water permeability test (WPT).

Table 1—Mixture design of concrete specimens

Constituents	Cement, lb/ft^3 (kg/m^3)	Water, lb/ft^3 (kg/m^3)	Fine aggregate, lb/ft^3 (kg/m^3)	Coarse aggregate, lb/ft^3 (kg/m^3)
Initial mixture design (w/c = 0.5)	22.22 (355.93)	11.11 (177.96)	52.96 (848.34)	64.44 (1032.23)
Adjusted mixture design (w/c = 0.71)	22.22 (355.93)	15.77 (252.71)	52.96 (848.34)	64.44 (1032.23)

For the test of residual compressive strength, 4 x 8 in. (101.60 x 203.20 mm) cylinders were used. Axial strains were measured using two extensometers that delivered an averaged axial deformation measurement. Displacement control with a rate of 0.0001 in./second (0.00254 mm/second) was used to capture the softening branch in the compression test.

Experimental parameters

The water permeability test (WPT) was performed after each specimen was subjected to one of the temperature scenarios used in the study. The experimental parameters were heating rates of 35.6 and 59 °F/minute (2 and 15 °C/minute), holding durations of 2 and 4 hours at each maximum target temperature, and cooling conditions, which included a slow cooling of 33.8 °F/minute (1 °C/minute), a natural cooling in the furnace, and a fast cooling in water. The maximum target temperatures were 392, 752, and 1112 °F (200, 400, and 600 °C). In this series of WPT tests, the maximum temperature 1472 °F (800 °C) was removed from the testing variables of

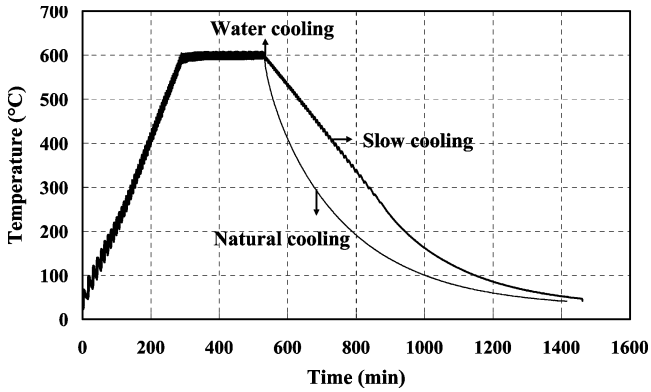

Fig. 3—Temperature histories for different cooling methods. (Note: °F = 1.8 × °C + 32.)

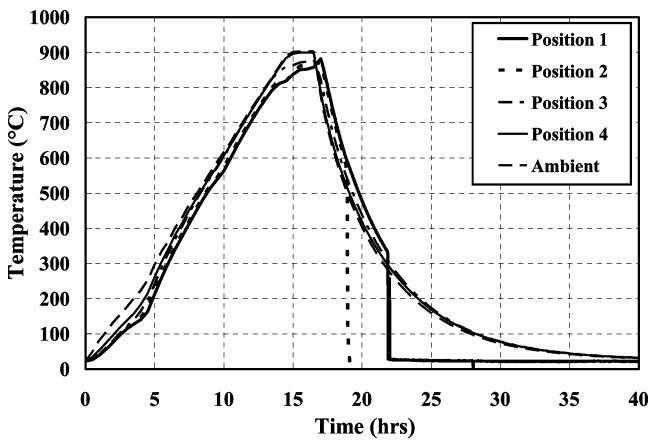

Fig. 4—Transient temperature histories in concrete cylinder. (Note: °F = 1.8 × °C + 32.)

the original test plan because the degree of damage in the specimens was very high, and the water flow through the damaged specimen was so rapid that the permeability could not be accurately measured.

For the series of residual compressive strength tests, the variables were three cooling conditions (the same slow cooling, natural cooling, and water cooling as for the WPT test series), and four maximum target temperatures 392, 752, 1112, and 1472 °F (200, 400, 600, and 800 °C). The heating rate was 35.6 °F/minute (2 °C/minute), while the holding time at the maximum temperature was 4 hours. In this study, the heating rates were not as high as specified in the standard fire curves ISO 834 (or BS 476) and ASTM E119 because of the limited heating capacity of our furnace.

The furnace was equipped with two groups of heating elements that were placed on opposite sides of the specimen. To provide uniform thermal conditions near the specimen, the concrete specimen was placed inside a hollow tube made of mullite with a maximum operational temperature of 3092 °F (1700 °C). Figure 3 shows the temperature histories using a heating rate of 35.6 °F/minute (2 °C/minute), a holding time of 4 hours at the maximum temperature of 1112 °F (600 °C), and three different cooling conditions. The temperature histories were recorded between the mullite tube and the concrete specimen using the K-thermocouple. In the cases of natural and slow cooling in Fig. 3, the specimen was left in the furnace until it cooled to the room temperature

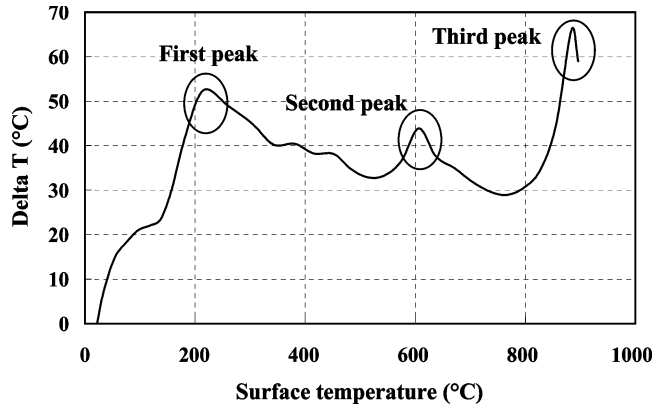

Fig. 5—ΔT (temperature difference between surface and center) versus surface temperature. (Note: °F = 1.8 × °C + 32.)

with a controlled cooling rate, and the temperature change was recorded over time. For water cooling, the specimen was taken out of the furnace and immediately put in a tank of water with an initial temperature of 68 °F (20 °C). The temperature of the specimen was expected to drop very quickly as soon as it is submerged in the water. As a result, the temperature drop inside the specimen could not be recorded for water cooling.

TEST RESULTS AND DISCUSSIONS

Internal temperature distributions and thermal diffusivity of concrete

Thermal diffusivity is one of the fundamental thermal properties of concrete. The thermal diffusivity was evaluated from internal temperature profiles obtained in 4 x 8 in. (101.60 x 203.20 mm) concrete cylinders. Figure 4 shows temperature histories over time measured at each thermocouple location. The two vertical drops during cooling, near 1004 °F (540 °C) at the center and near 626 °F (330 °C) at mid-radius, are due to the damage of the two thermocouples in Position 1 and Position 2.

Figure 5 shows the temperature difference between the surface and the center of the specimen during heating. One can see that the temperature difference varies during the entire testing period, which means that a steady state condition of uniform temperature was never reached. The three peaks shown in the figure are related to the microstructural changes due to complex physicochemical transformations in the concrete subjected to different temperatures. Most of the natural aggregates used in structural concrete are stable up to 500 °F (260 °C) and possibly well beyond this temperature, that is, they exhibit no chemical or phase transformations that could cause destructive volume changes or strength loss.[23] Thus, the peaks shown in Fig. 5 are closely related to chemical changes of hardened portland cement. The relationship between the peaks and the chemical changes of hardened cement paste may be explained on the basis of differential thermal analysis (DTA) conducted on hardened portland cement by Lankard.[23] The first peak occurs at 392 °F (200 °C). This peak is associated with the evaporation of free water, ettringite decomposition, and the beginning of calcium silicate hydrate (C-S-H) dehydration. In fact, the weight of the concrete specimen decreases rapidly up to 392 °F (200 °C) due to the evaporation of free water, which will be discussed later in conjunction with Fig. 6. The second peak between 1022 and 1202 °F (550 and 650 °C) is related to the decompositions of calcium hydroxide (CH) and C-S-H. The peak occurring

at 1562 °F (850 °C) is likely due to the decomposition of calcium carbonate ($CaCO_3$) observed in the DTA tests by Lankard.[23]

Figure 7 shows the temperature profiles measured at Positions 1, 2, and 3 when the temperature at the center of the specimen reached 1112 and 1472 °F (600 and 800 °C) during heating and cooling. The surface temperature corresponding to each temperature profile is indicated in the four plots. While undergoing natural cooling, the temperature difference between the center and the surface is two times larger than during heating. This is due to the fast cooling rate as compared with the heating rate of 33.8 °F/minute (1 °C/minute). The large temperature difference leads to a large temperature gradient, which has a strong effect on the damage of the mechanical properties (the decreases of strength and stiffness) and transport properties (the increase of water permeability), which will be discussed later.

One item of the important information that can be obtained from the temperature profiles shown in Fig. 7 is the thermal diffusivity of the cylindrical concrete specimens. A simplified expression was developed by Khoury et al.[9] assuming linear heat conduction in a solid cylinder subjected to a constant surface temperature increase. It relates the thermal diffusivity k_T to the temperature difference ΔT between the surface and the center of the test cylinder.

$$k_T = v_h R^2/4\Delta T \quad (1)$$

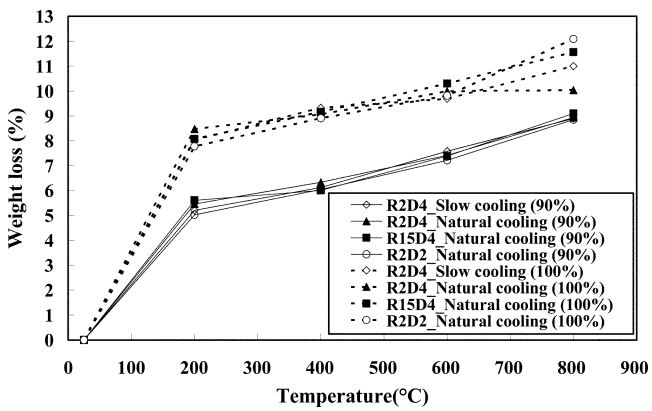

Fig. 6—Effect of heating on weight loss (RH = 90 and 100%). (Note: °F = 1.8 × °C + 32.)

where v_h denotes the rate of temperature change of the specimen at the surface and R denotes the radius of the cylinder, respectively. Note this expression does not account for the temperature dependence of the thermal diffusivity and for the coupling with simultaneous moisture transport.

Figure 8 is the plot of the thermal diffusivity calculated by using Khoury's expression in Eq. (1) and the temperature profiles shown in Fig. 7. One can see a large drop in the thermal diffusivity up to 392 °F (200 °C), which is primarily related to the loss of free water. Beyond this temperature the thermal diffusivity shows relatively little variation with increasing temperature up to 1472 °F (800°C).

Water permeability test (WPT) and coefficient of hydraulic permeability

The water permeability test was conducted for concrete specimens with different combinations of the testing variables. The results for the testing series R15D2_Natural cooling (heating rate R of 59 °F/minute [15 °C/minute], holding duration D of 2 hours at target temperatures, and natural cooling) are plotted in Fig. 9 for the cumulative water permeated, Q, versus time (minute). Q is the amount of cumulative water that permeates through the distressed concrete. In this study, we studied the effects of different target temperatures on the water permeated with the same rate of cooling; and the effects of different cooling methods on the water permeated with the same target temperature. The cumulative water permeated, Q, and the rate of $Q(dQ/dt)$ are measures of thermal damage in the concrete. A higher Q value (or a higher slope) indicates more damage in the concrete. The test results indicated that the initial slope of cumulative water flowing through the specimen greatly increases as the target temperature increases beyond 752 °F (400 °C), and that the initial slope of cumulative water flowing through the specimen drastically increases for water cooling. For the WPT tests, only one specimen for each combination of the testing variables was used because of the limited capacity of the furnace (only one specimen can be placed in the chamber) and long duration of permeability tests.

The cumulative water Q can be used to evaluate the hydraulic permeability of concrete. In fact, the coefficient of hydraulic permeability can be obtained from Darcy's law

$$V = K_p Ah/L \quad (2)$$

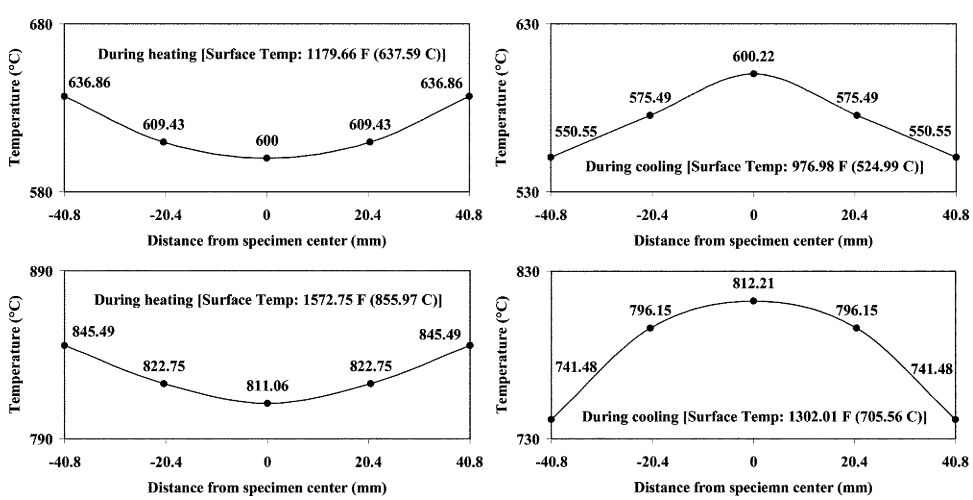

Fig. 7—Temperature profiles during heating and cooling. (Note: °F = 1.8 × °C + 32.)

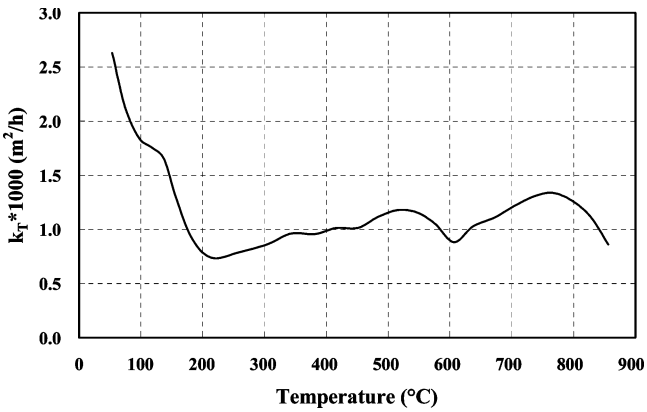

Fig. 8—Variation of thermal diffusivity with temperatures. (Note: 1 m^2 = 10.76 ft^2;°F = 1.8 × °C + 32.)

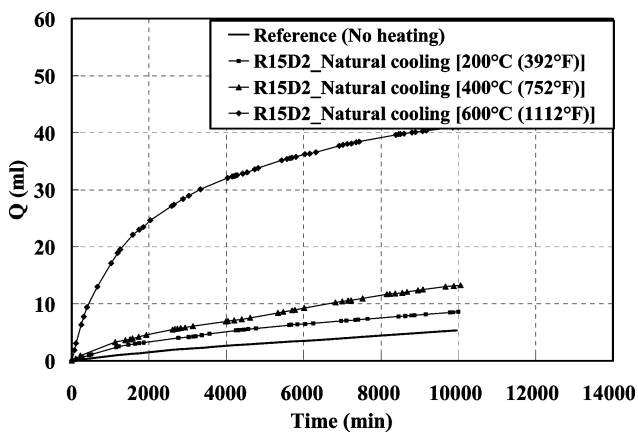

Fig. 9—Cumulative water permeated, Q*, versus time for R15D2_Natural cooling. (Note: 1 mL = 0.033814 oz.)*

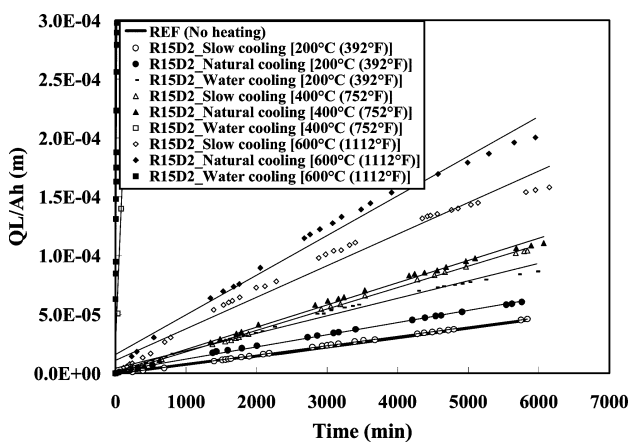

Fig. 10—Linear regression (Test Series R15D2) (Note: 1 m = 3.28 ft.)

Integrating this equation, one obtains

$$Q \cdot L/(A \cdot h) = K_p \cdot t \tag{3}$$

where V is the rate of flow (dQ/dt) per unit area (m/second); Q is the total water permeated (m^3); A is the cross section of the specimen (m^3); L is the thickness (m); h is the head of water (m); and K_p is the coefficient of permeability (m/second). Note that A and L in the specimens are constants, and the head h is assumed to remain constant if small differences in the pressure head during the test are neglected.

Table 2—Coefficients of water permeability for R15D2* test series

Temperature, °F (°C)	K_p, × 10^{-10} ft/s (× 10^{-10} m/s)		
	Slow cooling	Natural cooling	Water cooling
77 (25)	4.20 (1.28)	4.20 (1.28)	4.20 (1.28)
392 (200)	4.36 (1.33)	5.64 (1.72)	8.14 (2.48)
752 (400)	9.94 (3.03)	10.33 (3.15)	776.48 (236.67)
1112 (600)	14.67 (4.47)	18.44 (5.62)	7928.71 (2416.67)

*Heating rate R for R15D2 = 59 °F/minute (15 °C/minute) and 2-hour holding duration D at target temperatures.

Table 3—Coefficients of water permeability for R2D4* test series

Temperature, °F (°C)	K_p, × 10^{-10} ft/s (× 10^{-10} m/s)		
	Slow cooling	Natural cooling	Water cooling
77 (25)	4.20 (1.28)	4.20 (1.28)	4.20 (1.28)
392 (200)	4.72 (1.44)	5.97 (1.82)	12.24 (3.73)
752 (400)	7.61 (2.32)	8.37 (2.55)	1438.09 (438.33)
1112 (600)	10.33 (3.15)	12.63 (3.85)	10,722.08 (3283.33)

*Heating rate R for R2D4 = 35.6 °F/minute (2 °C/minute) and 4-hour holding duration D at target temperatures.

Figure 10 (Test Series R15D2) is a plot of the linear regression of $Q \cdot L/(A \cdot h)$ versus time when steady state flow is established. The coefficient of permeability K_p is then calculated from the slope found from the linear regression. Tables 2 and 3 show the values of the coefficient of permeability for Test Series R15D2 and R2D4, respectively. From Tables 2 and 3, one can see that the value of K_p increases when the specimen is subjected to higher temperatures and faster cooling rates. These results mean that a higher heating temperature causes more damage in the concrete and thus results in a higher residual permeability of the distressed concrete. More importantly, these results indicate that a faster cooling rate (corresponding to a higher internal temperature gradient) causes more damage in the concrete and thus results in a higher residual permeability of the distressed concrete. Particularly, the K_p values of the specimens subjected to the target temperatures 752 and 1112 °F (400 and 600 °C) underwater cooling are much higher than those subjected to other cooling methods (natural cooling and slow cooling). Columns 1 and 2 of Tables 2 and 3 show that, under slow and natural cooling, the permeability increases far less than under water cooling.

Figures 11 and 12 plot the test data by using relative water permeability, which is the ratio of the permeability coefficient of the heated specimen and that of the reference specimen (not heated). These two figures show the relative water permeability up to the maximum temperature for the Test Series R15D2 and R2D4, respectively, which clearly illustrate the effects of target temperature and cooling rate. Comparing Fig. 11 and 12, for the specimens exposed to the target temperatures over 752 °F (400 °C), it is obvious that the effect of the holding time on the coefficients of permeability is not as significant as the heating rate. In the lower temperature ranges, up to a target temperature of 392 °F (200 °C), the

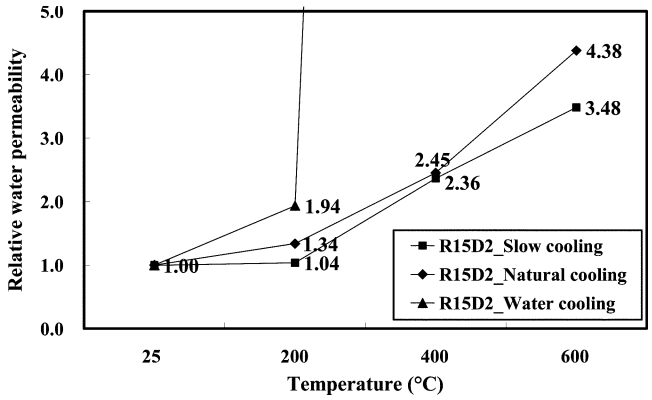

Fig. 11—Relative water permeability (Test Series R15D2). (Note: °F = 1.8 × °C + 32.)

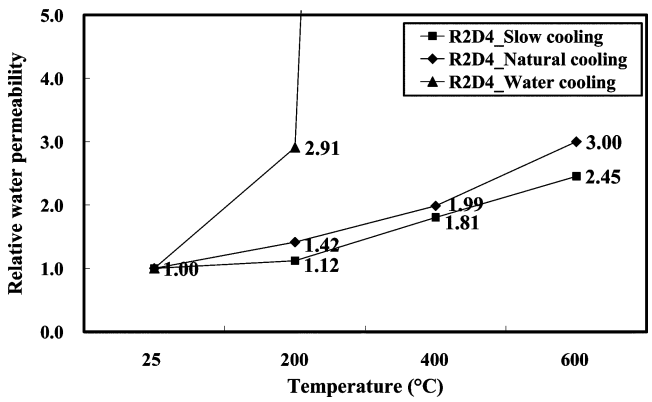

Fig. 12—Relative water permeability (Test Series R2D4). (Note: °F = 1.8 × °C + 32.)

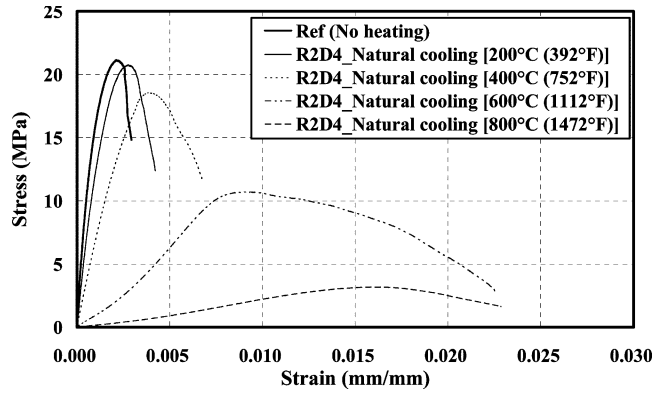

Fig. 13—Stress-strain curves for R2D4_Natural cooling. (Note: 1 MPa = 145.04 psi.)

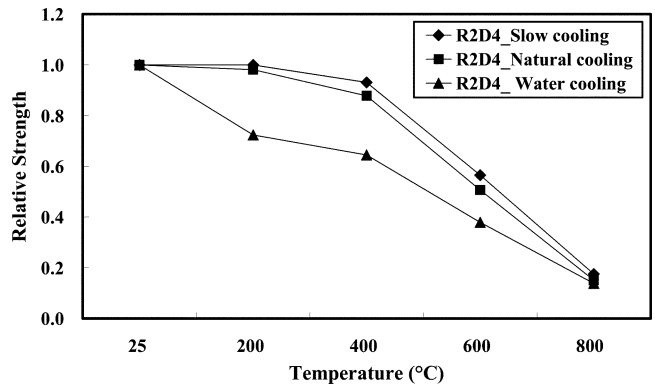

Fig. 14—Relative ultimate residual strength versus maximum temperature. (Note: °F = 1.8 × °C + 32.)

difference between the two effects (heating rate and holding duration) is not significant.

In the past, strength and stiffness reductions of concrete due to fire have been considered as major indicators for evaluating fire damage of concrete. The present results show that the residual permeability is actually more sensitive to high temperature parameters, such as target temperature and cooling rate. Therefore, the water permeability can be used as a parameter to evaluate residual transport properties (and durability) of fire-damaged concrete. Both target temperature and cooling rate should be considered as important factors affecting the post-fire transport properties of concrete.

Residual compressive strength and modulus of elasticity

Figure 13 plots compressive stress-versus-strain curves for the specimens that were subjected to different target temperatures and natural cooling. The stress-strain curves obtained with slow and natural cooling methods showed similar trends as those in Fig. 13. As shown in the figure, the compressive strength and modulus of elasticity decrease significantly as the maximum target temperature increases. Figure 14 shows the residual ultimate strength normalized by the reference strength (obtained at 77 °F [25 °C)]) for three cooling methods as a function of the target temperatures. The residual strength drops rapidly when the target temperature increases beyond 752 °F (400 °C). The strength of the specimens subjected to water cooling decreases more rapidly than the specimens subjected to other cooling methods. The strength of specimens exposed to the target temperature of 1112 °F (600 °C) is less than 57% of the reference strength tested at the room temperature. For 1472 °F (800 °C), the strength is less than 18% of the reference strength.

Figure 15 shows the values of the initial tangent modulus with different temperatures, normalized by the reference specimen tested at room temperature. The basic trend of the initial tangent modulus is similar to that of the residual strength shown in Fig. 14. The initial tangent modulus of concrete, however, is more sensitive to elevated temperatures than the compressive strength. The initial tangent modulus of the specimens exposed to a maximum temperature of 1112 °F (600 °C) is less than 5.3% of the initial reference tangent modulus. For 1472 °F (800 °C), the initial tangent modulus is less than 1.3% of the reference values. Therefore, the results demonstrate that faster cooling results in more rapid decrease of both strength and stiffness properties of concrete.

Weight loss

To study the effect of initial relative humidity (RH) on the weight loss of concrete under different temperatures, two initial values of RH, 90 and 100%, were used in this study. The specimens were concrete slices of 4 (diameter) x 2 in. (thickness) (101.6 x 50.8 mm). The specimens with 90% initial RH were cured under the standard condition (temperature 73.4 °F [23 °C] and RH 93%) for 8 weeks. The fully saturated specimens were submerged in a water tank

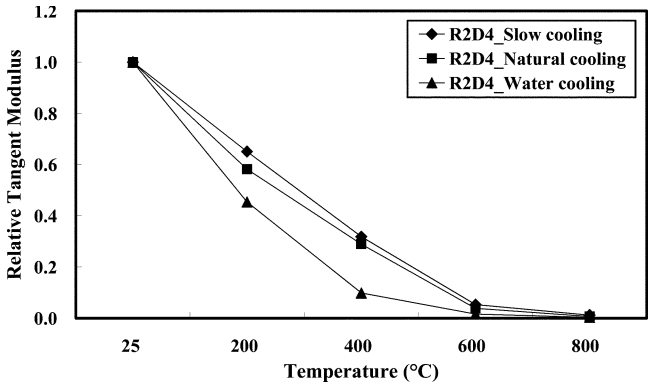

Fig. 15—Relative initial tangent modulus versus maximum temperature. (Note: °F = 1.8 × °C + 32.)

(68 °F [20 °C]) for 3 days after curing under the same condition as the specimens with 90% RH.

The weight loss measurement did not include water cooling specimens because they were submerged in water immediately after the high temperature treatment. The weight losses for both initial RH 90 and 100% are plotted in Fig. 6 for Series R2D2 (heating rate *R* of 35.6 °F/minute [2 °C/minute] and holding duration *D* of 2 hours at target temperatures), R2D4, and R15D4, respectively.

In general, the weight loss increases with increasing target temperature. The weight loss and the target temperature, however, are not proportional over the entire temperature range. The slope of the weight loss versus temperature above 392 °F (200 °C) is considerably less than that in the range of 77 to 392 °F (25 to 200 °C), which is due to different mechanisms of weight loss. In the lower temperature range, the weight loss is due mainly to the evaporation of the free water present in the voids and capillary pores. After the evaporation of all free water, further weight loss comes from the removal of the adsorbed water in smaller pores, which takes more energy. Moreover, at high temperature, some phase transformations take place and a certain amount of chemically bound water is released and evaporated. The amount of adsorbed water and chemically bound water released due to the phase transformation is less than the free water in the concrete specimens with 90 and 100% initial RH. This leads to the reduced slope in the weight loss curves above 392 °F (200 °C).

The initial weight loss of fully saturated specimens is steeper than those for RH 90% specimens up to 392 °F (200 °C). This is because the fully saturated specimens contain more free water than the specimens of RH 90%. At temperatures higher than 392 °F (200 °C), the slopes for both types of specimens are almost the same. This means that the evaporation of the free water in the voids and capillary pores is almost complete at a temperature of 392 °F (200 °C). Therefore, regardless of the initial moisture content of concrete, after 392 °F (200 °C), the rate of weight loss is similar for all specimens. The constant slope after 392 °F (200 °C) indicates that the weight loss of concrete is governed by the same mechanism from 392 °F (200 °C) up to 1472 °F (800 °C).

The test results for both 90 and 100% RH show that the weight loss is governed primarily by the target temperature, not by the heating rate, the cooling method, or the holding time (2 hours and 4 hours in this research).

CONCLUSIONS

1. The temperature difference between the surface and center of cylindrical concrete specimens varies during the entire testing period, including the holding time of 2 hours at the maximum target temperature. This means that a steady state temperature condition in the concrete is never reached;

2. Under continuous heating conditions, the temperature difference between the surface and center of the specimen exhibit three peaks in three different temperature ranges. The three peaks are related to phase transformations in the hardened cement: the evaporation of free water around 392 °F (200 °C), the decomposition of calcium hydroxide (CH) and calcium silicate hydrate (C-S-H) between 1022 and 1202 °F (550 and 650 °C), and the decomposition of calcium carbonate ($CaCO_3$) above 1202 °F (650 °C);

3. Using the temperature difference between the center and the surface, thermal diffusivity of the concrete under different temperature ranges was obtained. The thermal diffusivity decreases from room temperature to 392 °F (200 °C), and it shows relatively little variation with increasing temperature up to 1472 °F (800 °C);

4. While undergoing natural cooling, the temperature difference between the center and the surface is two times larger than during heating. This means that even for natural cooling, the interior temperature gradient of the concrete specimen is higher than that during the heating process. This explains why the degradations in mechanical and transport properties of concrete are strongly affected by cooling methods;

5. Both the residual strength and stiffness of concrete decrease significantly as the cooling rate and the maximum temperature increase. Cooling rate is a very important parameter that is responsible for the fire-induced damage of concrete;

6. Water permeabilities of concrete specimens subjected to different heating and cooling treatments were measured. For the specimens exposed to the maximum temperature 392, 752, and 1112 °F (200, 400, and 600 °C), the water permeability increases significantly with increasing target temperature and cooling rates. Therefore, the water permeability can be used as an experimental parameter to evaluate residual transport properties (and durability) of fire-damaged concrete;

7. For the concrete specimens subjected to slow or natural cooling, the effect of the heating rate on the water permeability is more significant than the effect of holding time;

8. For concrete specimens with 90% initial relative humidity and full saturation, the weight loss below 392 °F (200 °C) is far larger than that above 392 °F (200 °C). The weight loss in this temperature range is governed by the evaporation of the free water. The weight loss at temperatures above 392 °F (200 °C) is due to the loss of adsorbed and chemically bound water in the specimen. The weight loss is governed by the exposed maximum temperature rather than the heating rate, cooling method, and holding time (2 and 4 hours in this research).

ACKNOWLEDGMENTS

The authors wish to acknowledge partial support by the U.S. National Science Foundation under Grant CMS-0409747 to the University of Colorado at Boulder. Opinions expressed in this paper are those of the authors and do not necessarily reflect those of the sponsor. The authors also thank E. Sheesley for his work in editing this paper.

REFERENCES

1. Abrams, M. S., "Compressive Strength of Concrete at Temperatures to 1600 °F," *Temperature and Concrete*, SP-25, American Concrete Institute, Farmington Hills, MI, 1971, pp. 33-58.

2. Bažant, Z., and Kaplan, M. F., *Concrete at High Temperatures, Material Properties, and Mathematical Models*, second edition, Pearson Education, Edinburgh, UK, 2002.

3. Castillo, C., and Durani, A. J., "Effect of Transient High Temperature on High-Strength Concrete," *ACI Materials Journal*, V. 87, No. 1, Jan.-Feb. 1990, pp. 38-67.

4. Cheng, F. P.; Kodur, V. K. R.; and Wang, T. C., "Stress-Strain Curves for High Strength Concrete at Elevated Temperature," *Journal of Materials in Civil Engineering*, ASCE, V. 16, No. 1, 2004, pp. 84-90.

5. Felicetti, R., and Gambarova, P. G., "Heat in Concrete: Special Issues in Materials Testing," *Studies and Researches*, Graduate School in Concrete Structures—Fratelli Pesenti Politecnico di Milano, Italy, V. 24, 2003, pp. 121-138.

6. Furumura, F.; Abe, T.; and Shinohara, Y., "Mechanical Properties of High Strength Concrete at High Temperature," *Proceedings of the Fourth Weimar Workshop on High Performance Concrete: Material Properties and Design*, Hochschule fuer Architektur und Bauwesen (HAB), Weimar, Germany, 1995, pp. 237-254.

7. Guo, J. S., and Waldron, P., "Development of the Stiffness Damage Test (SDT) for Characterization of Thermally Loaded Concrete," *Materials and Structures*, RILEM, V. 33, No. 8, 2000, pp. 483-491.

8. Khoury, G. A.; Sullivan, P. J. E.; and Grainger, B. N., "Strain of Concrete during First Heating to 600 °C under Load," *Magazine of Concrete Research*, V. 37, No. 133, 1985, pp. 195-215.

9. Khoury, G. A.; Sullivan, P. J. E.; and Grainger, B. N., "Transient Thermal Strain of Concrete: Literature Review, Conditions within Specimen and Individual Constituent Behavior," *Magazine of Concrete Research*, V. 37, No. 132, 1985, pp. 131-144.

10. Khoury, G. A.; Grainger, B. N.; and Sullivan, P. J. E., "Strain of Concrete during First Cooling to 600 °C under Load," *Magazine of Concrete Research*, V. 38, No. 134, 1986, pp. 3-12.

11. Kodur, V. K. R., and Sultan, M. A., "Effect of Temperature on Thermal Properties of High-Strength Concrete," *Journal of Materials in Civil Engineering*, ASCE, V. 15, No. 2, Mar.-Apr. 2003, pp. 101-107.

12. Leithner, D., "Experimental Investigation of Concrete Subjected to Fire Loading," diploma thesis, Technical University Vienna, Vienna, Austria, 2004.

13. Luo, X.; Sun, W.; and Chen, S. Y. N., "Effect of Heating and Cooling Regimes on Residual Strength and Microstructure of Normal Strength and High-Performance Concrete," *Cement and Concrete Research*, V. 30, No. 3, 2000, pp. 379-383.

14. Phan, L. T., "Fire Performance of High-Strength Concrete: A Report of the State-of-the Art, Building and Fire Research Laboratory," NISTIR 5934, National Institute of Standards and Technology, Dec. 1996.

15. Phan, L. T., and Carino, N. J., "Review of Mechanical Properties of HSC at Elevated Temperature," *Journal of Materials in Civil Engineering*, ASCE, V. 10, No. 1, 1998, pp. 58-64.

16. Phan, L. T.; Lawson, J. R.; and Davis, F. L., "Effect of Elevated Temperature Exposure on Heating Characteristics, Spalling, and Residual Properties of High Performance Concrete," *Materials and Structures*, RILEM, V. 34, No. 2, 2001, pp. 83-91.

17. Phan, L. T., "High-Strength Concrete at High Temperature—An Overview," *Utilization of High Strength/High Performance Concrete*, 6th International Symposium, Leipzig, Germany, V. 1, 2002, pp. 501-518.

18. Poon, C. S.; Azhar, S.; Anson, M.; and Wong, Y. L., "Comparison of the Strength and Durability Performance of Normal- and High-Strength Pozzolanic Concretes at Elevated Temperatures," *Cement and Concrete Research*, V. 31, No. 9, 2001, pp. 1291-1300.

19. Schneider, U., "Concrete at High Temperatures—A General Review," *Fire Safety Journal*, V. 13, No. 1, 1988, pp. 55-68.

20. Ravindrarajah, R. S.; Lopez, R.; and Reslan, H., "Effect of Elevated Temperature on the Properties of High-Strength Concrete Containing Cement Supplementary Materials," 9th International Conference on Durability of Building Materials and Components, Australia, Mar. 2002.

21. Reis, M. L. B. C.; Neves, I. C.; Tadeu, A. J. B.; and Rodrigues, J. P. C., "High-Temperature Compressive Strength of Steel Fiber High-Strength Concrete," *Journal of Materials in Civil Engineering*, ASCE, V. 13, No. 3, 2001, pp. 230-234.

22. Ludirdja, D.; Berger, R. L.; and Young, J. F., "Simple Method for Measuring Water Permeability of Concrete," *ACI Materials Journal*, V. 86, No. 5, Sept.-Oct. 1989, pp. 433-439.

23. Lankard, D. R., "The Dimensional Instability of Heated Portland Cement Concrete," PhD dissertation, Ohio State University, Cleveland, OH, 1970.

Reproduced with permission of the copyright owner. Further reproduction prohibited without permission.